Pergamon

Chemical Engineering Science, Vol. 53, No. 15, pp. 2823–2837, 1998

Printed in Great Britain

PII: S0009–2509(98)00099–2

0009–2509/98/$–See front matter

Stability of evaporating two-layered liquid film in the presence of surfactant—II. Linear analysis

Krassimir D. Danov,* Vesselin N. Paunov,* Simeon D. Stoyanov,* Norbert Alleborn,†‡ Hans Raszillier† and Franz Durst

* Laboratory of Thermodynamics and Physicochemical Hydrodynamics, Faculty of Chemistry, Sofia University, 1 J. Bourchier Ave., 1126 Sofia, Bulgaria

† Lehrstuhl für Strömungsmechanik, Universität Erlangen-Nürnberg, Cauerstr. 4, D-91058 Erlangen, Germany

(Received 17 April 1997)

Abstract—In this study we perform a linear analysis of the stability of a two-layered liquid film which is evaporating upon a horizontal solid substrate. The film contains surfactant that is soluble in both liquid phases. The problem was solved in general form, in our previous work [cf. Danov *et al.* (1997b) *Chem. Engng Sci.*, submitted] by using lubrication approximation. The governing equations for the film thickness and the surfactant concentration derived there are treated using linear analysis in the present study. The resulting system of ordinary differential equations describes the evolution of small long-wave disturbances of the film shape and the surfactant distribution during the film evaporation. The model allows one to investigate the role of different factors on the film stability. To illustrate the effects we consider a particular system: water–hexane film evaporating on a PVC plate. The limiting cases of pure liquids and tangentially immobile surfaces, as well as the general case are studied numerically. Both cases when a low- and a high-molecular weight surfactants present into the film are investigated. The numerical results in the case of non-linear stability analysis of a PVC/tetrachlorethane/water/vapour evaporating film are subject of part III [cf. Paunov *et al.* (1997) *Chem. Engng Sci.*, submitted].

Keywords: Liquid film; stability; evaporation; two layers; soluble surfactant.

1. INTRODUCTION

The stability of thin liquid films under condition of evaporation is a problem of great importance from both technological and scientific point of view. The modern coating technology often requires a simultaneous coating with multilayered films which undergo further evaporation. The quality of the coatings produced depends strongly on the stability of the multilayered liquid film against outer mechanical and thermal disturbances. The stability mechanism in multilayered liquid films depends strongly on the particular system. The attractive disjoining pressure and the processes like evaporation or condensation of vapour at the interface can amplify the disturbance in the film shape which leads to the film rupture. When surfactant is present in the system at low concentration it can cause a destabilising effect due to Marangoni instability. On the contrary, at high surfactant concentration (close or above the critical micelles concentration) the surfactant can have a stabilising effect due to the suppression of capillary waves at the film surfaces. For detailed literature review of the contributions to the stability analysis of thin liquid films see Danov *et al.* (1997a, b).

In this study we deal with the problem of the stability of evaporating two-layered liquid films that contain a dissolved surfactant. The film is attached to a heated solid substrate. Closely related to the present study is the work by Danov *et al.* (1997a) where the linear stability of a single evaporating film on a heated solid substrate has been considered. The presence of surfactant has also been taken into account.

In Part I of the present study (cf. Danov *et al.*, 1997b), we extended the model of Danov *et al.* (1997a) by taking into account the presence of a second liquid layer. We investigated the evolution of long waves on both liquid interfaces by using lubrication approximation, and we derived a system of three partial differential equations governing the evolution of the disturbances of the film shape and of the surfactant concentration. Due to the large number of dimensionless groups appearing in the problem, it is practically impossible to perform a complete parametric study in

‡ Corresponding author.

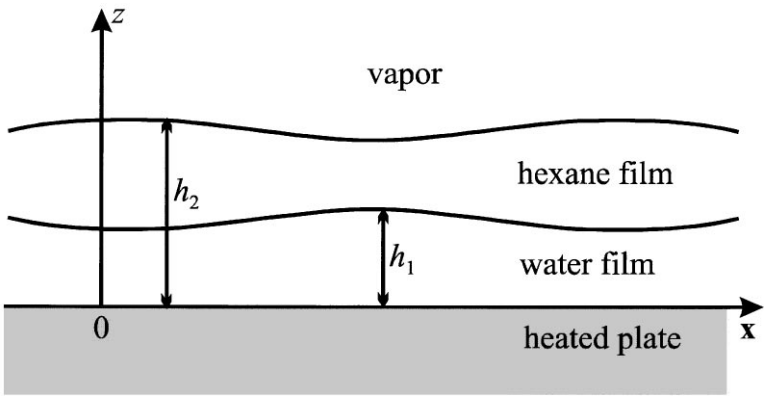

Fig. 1. The physical configuration of the two-layered film on a heated plate.

the general case, moreover, no physical system corresponds to each combination of dimensionless numbers. In general, there are two typical configurations of two-layered films. These are the cases of water-light oil film and heavy oil–water film that often appear in practice. For this reason we split the numerical analysis of the stability of two-layered films in two separate papers, considering there particular physical systems.

Here, in Part II of the study, we perform a *linear stability analysis* of the system of evaporating water–hexane film in the presence of surfactant, presented in Danov *et al.* (1997b). *Non-linear stability analysis* of the complementary case of tetrachlorethane–water film is a subject of Part III of this study (cf. Paunov *et al.*, 1997).

2. CONFIGURATION AND BASIC STATE OF THE SYSTEM

Let us consider an evaporating two-layered film in the presence of surfactant—see Fig. 1. In Danov *et al.* (1997b) we derived the system of three partial differential equation [eqs (44), (45) and (59) therein] governing the evolution of the profiles of the two layers and the surfactant concentration. Here we will linearise the governing equations for small deviation from the basic state (without fluctuations). All the notations and the dimensionless groups appearing below are defined in a similar way as in Danov *et al.* (1997b), which allows one to keep them fixed during the process of evaporation, when both the temperature and the surfactant concentration change. The numerical analysis of the dimensionless groups for the physical parameters of the same system (PVC/water/hexane/vapour film) is performed therein. Here we work with the same values of the physical parameters and of the respective dimensionless numbers. In this case, the expressions for van der Waals disjoining pressures, $\Pi_1$and Π_2, in the two liquid films read

$$\Pi_1 = -\frac{A_1}{6\pi h_{\text{low}}^3} - \frac{A_i}{6\pi(h_{\text{low}}+h_0)^3},$$
$$\Pi_2 = -\frac{A_2}{6\pi h_0^3} - \frac{A_i}{6\pi(h_{\text{low}}+h_0)^3} \qquad (1)$$

where h_{low} and h_0 are the local thicknesses of the water and hexane films, respectively. As calculated in Danov *et al.* (1997b), the values of the Hamaker constants for that system are $A_1 = 5.9\times10^{-21}$ J, $A_2 = 5.2\times10^{-21}$ J, and $A_i = -9.3\times10^{-21}$ J. One sees that for small film thickness the van der Waals disjoining pressure in both liquid films is attractive and can amplify the film shape fluctuations. For an illustration we have plotted in Figs 2(a) and (b) the van der Waals disjoining pressure in the water and in the hexane film, respectively. The different curves correspond to different thicknesses of the other liquid film. It is worth mentioning that the second term in eq. (1) is repulsive, but it dominates only at very large film thickness where the disjoining pressure effect is negligible. Hence the surface forces in this case can only destabilise the two-layered film.

We assume that the unperturbed state of the film corresponds to flat film interfaces of time-dependent thickness of the evaporating hexane film, $H_{2,b}$ (dimensionless), and time-independent thickness of the water film, $H_{1,b} = h_{12}$. Here h_{12} is the initial thickness ratio of the water and hexane film. The basic state quantities will be denoted further by a subscript b. Then the solution of the compatibility equations (44) and (45) derived in Danov *et al.* (1997b) can be written in the following form:

$$H_{2,b} = \sqrt{(\mathscr{K}+h_{12}\lambda_{21})^2 + [2(\mathscr{K}+h_{12}\lambda_{21})+1](1-\tau)} - (\mathscr{K}+h_{12}\lambda_{21}). \qquad (2)$$

The time for which zero thickness of the evaporating layer is achieved without any fluctuations is called disappearance time t_d in the literature; it corresponds to the dimensionless time, $\tau = 1(\tau \equiv t/t_d)$. Here $\mathscr{K}$ is a dimensionless number, characterising the degree of non-equilibrium at the evaporating interface (see Danov *et al.*, 1997a for details); λ_{21} is the ratio of the two films thermal conductivities. As a rule, due to instabilities the evaporating thin liquid films rupture at a time earlier than t_d. The basic state of the mass flux [see eq. (2.4) in Danov *et al.* (1997b)] at the

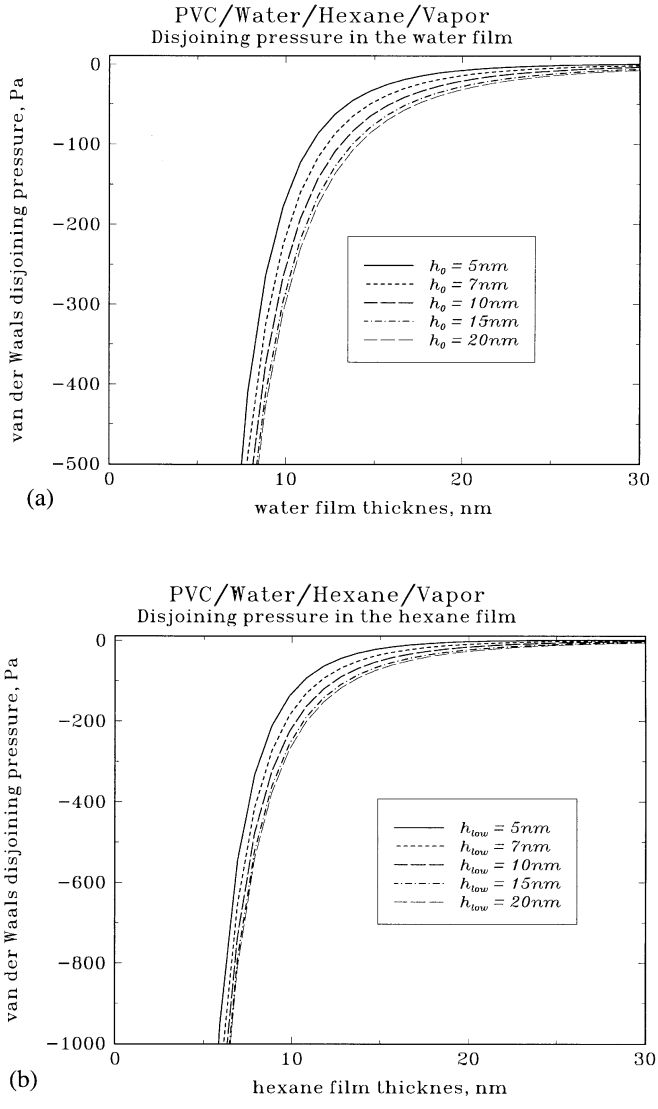

Fig. 2. Dependence of the dimensional van der Waals disjoining pressure on the film thickness: (a) for the water film; the different curves correspond to different thicknesses, h_0, of the upper (hexane) film; (b) for the hexane film, the different curves correspond to different thicknesses, h_{low}, of the lower (water) film. The values of the Hamaker constants are as follows: $A_1 = 5.9 \times 10^{-21}$ J, $A_2 = 5.2 \times 10^{-21}$ J, and $A_i = -9.3 \times 10^{-21}$ J.

interface corresponding to our eq. (2) reads

$$\frac{J_b}{J_T \Delta T} = \frac{\mathscr{K}}{\sqrt{(\mathscr{K} + h_{12}\lambda_{21})^2 + [2(\mathscr{K} + h_{12}\lambda_{21}) + 1](1 - \tau)}}. \tag{3}$$

The behaviour of the basic state for various degrees of non-equilibrium evaporation is principally the same as in the absence of the second layer. The presence of the second layer increases $\mathscr{K}$ to $\mathscr{K} + h_{12}\lambda_{21}$ (cf. Danov *et al.*, 1997a). From eq. (3) it follows that the mass flux increases in time, in the first stage not so pronounced, but with decreasing film thickness the intensity of evaporation increases significantly. The presence of the second layer decreases the mass loss and it can be negligible for $\mathscr{K} \ll h_{12}\lambda_{21}$.

The effect of the second layer on the behaviour of the basic state thickness of the hexane film (for various thicknesses of the water film) is illustrated in Fig. 3. The increase in water film thickness decreases the disappearance velocity and the evaporating film thickness changes slowly in a real dimensionless time $tJ_TL/(\rho_2 h_0)$. Hence, for a given constant degree of non-equilibrium, the increase of the thermal capacity of the layer between the solid substrate and evaporating film prevents the evaporation due to the decrease of the evaporation mass flux.

From eq. (59) in Danov *et al.* (1997b) we derive the basic state for the dimensionless adsorptions $G_{1,b}$ and $G_{2,b}$, and bulk concentration, C_b, of

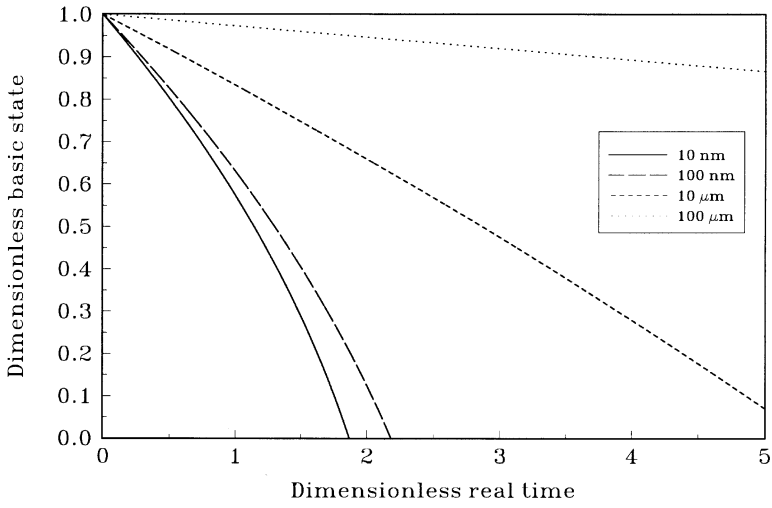

Fig. 3. Dependence of the dimensionless basic state hexane film thickness for $h_0 = 10$ nm and different water film thicknesses $h_w = 10$, 100 nm, 1, 10 μm vs. the real dimensionless time $tJ_T L/(\rho_2 h_0)$.

surfactant:

$$\Gamma_{12}G_{1,b} + G_{2,b} + \mathscr{Z}_2(H_{2,b} + m_{21}h_{12})C_b = \Gamma_{12}G_{1,b}(0) + G_{2,b}(0) + \mathscr{Z}_2(1 + m_{21}h_{12})C_b(0). \quad (4)$$

Here $\mathscr{Z}_2$ is the surfactant capacity number of the hexane layer; and Γ_{12} is the ratio of the surfactant adsorption at the two liquid interfaces when the bulk concentration is equal to CMC (see Danov *et al.*, 1997b for details). Equation (4) expresses the conservation of the total surfactant mass in the film. Due to the evaporation the thickness of the upper layer decreases, the concentration of surfactant increases in both layers and hence the adsorption increases. If the initial amount of the surfactant is large enough, then in the liquid phase of smaller CMC the final value of adsorption will be achieved earlier. Then, the surfactant transfer to this phase will not increase the adsorption at the interfaces any more and all the incoming surfactant will form micelles. In this case, the mobility of interfaces due to the process of evaporation can change in a complicated way, depending on the ratio of CMC values of the surfactant in the two liquid phases and the surfactant distribution coefficient m_{21}.

3. LINEAR STABILITY ANALYSIS

To perform a linear analysis of the governing system of equations derived in the first part of this study (cf. Danov *et al.*, 1997b), we introduce small fluctuations in the dimensionless pressure P_i, the interfacial velocity $\mathbf{U}_i$, the shape H_i, the adsorption G_i, and the surfactant concentration C. (Here i is equal to 1 for the lower phase and i is equal to 2 for the upper phase.) For the sake of simplicity, we consider only planar surface waves with a dimensionless wave number k and lateral wave functions $\cos(kx)$ and $\sin(kx)$. The perturbed physical parameters of the problem can be put in the form

$$H_i = H_{i,b}[1 + H_{i,f}\cos(kx)], \quad P_i = P_{i,b} + P_{i,f}\cos(kx),$$
$$U_i = U_{i,f}\sin(kx), \quad G_i = G_{i,b} + G_{i,f}\cos(kx),$$
$$C = C_b + C_f\cos(kx) \quad (5)$$

where the perturbation amplitudes are denoted by subscript f; they depend only on the dimensionless time τ. The perturbation amplitude $H_{2,f}$ of the shape of the evaporating surface is defined relative to the layer thickness $H_{2,b}$ of the basic state, which decreases in time due to evaporation. The corresponding perturbation amplitude $H_{1,f}$ of the lower liquid layer thickness is proportional to the constant h_{12}. The rupture time of the film is defined as the time at which one of the perturbation amplitudes of the layer thickness becomes equal to 1.

Note that $H_{1,f}$ and $H_{2,f}$ can have both different and equal signs which corresponds to different coupling of the instability modes of the two interfaces. The case $H_{1,f}H_{2,f} < 0$ corresponds to the so-called squeezing mode, whilst in the opposite case $H_{1,f}H_{2,f} > 0$ defines the bending mode. It is known that the squeezing mode disturbances for symmetric films give a larger contribution to the film instability than the bending mode disturbances (cf. Edwards *et al.*, 1991). This is a new element which is not present in the case of single film on a solid substrate (cf. Danov *et al.*, 1997a).

The linearised form of normal stress boundary conditions (52) and (53) in Danov *et al.* (1997b) give an explicit relation between the pressure amplitudes to the shape amplitudes

$$P_{1,f} = p_{h,11}H_{1,f} + p_{h,12}H_{2,f},$$
$$P_{2,f} = p_{h,21}H_{1,f} + p_{h,22}H_{2,f}. \quad (6)$$

Using eq. (5) the tangential stress boundary conditions presented by eqs (55) and (57) of Danov *et al.*

(1997b) can be transformed into a linear relation between the velocity amplitudes and shape and concentration amplitudes:

$$U_{1,f} = u_{h,11}H_{1,f} + u_{h,12}H_{2,f} + u_{c,1}C_f$$
$$U_{2,f} = u_{h,21}H_{1,f} + u_{h,22}H_{2,f} + u_{c,2}C_f. \quad (7)$$

Here and in eq. (6) the coefficients depend on the basic state [see Appendix A for details, eqs (A1)–(A5)].

The linearisation of the dimensionless Langmuir isotherm (49) in Danov *et al.* (1997b) leads to the simple linear relation between the fluctuations of the adsorption and concentration $G_{k,f} = g_k C_f$, where the coefficients g_k are defined by

$$g_1 = \frac{(1-\mathscr{G}_1)C_{12}m_{21}}{[(1-\mathscr{G}_1)C_{12}m_{21} + C_b\mathscr{G}_1]^2},$$
$$g_2 = \frac{1-\mathscr{G}_2}{(1-\mathscr{G}_2 + C_b\mathscr{G}_2)^2}. \quad (8)$$

The linearised form of the compatibility equations and the surfactant mass balance equation in the general case [see eqs (44), (45) and (59) in Danov *et al.* (1997b)] can be presented as follows:

$$\frac{dH_{1,f}}{d\tau} = a_{11}H_{1,f} + a_{12}H_{2,f} + a_{13}S_f \quad (9)$$

$$\frac{dH_{2,f}}{d\tau} = a_{21}H_{1,f} + a_{22}H_{2,f} + a_{23}S_f \quad (10)$$

$$\frac{dS_f}{d\tau} = a_{31}H_{1,f} + a_{32}H_{2,f} + a_{33}S_f \quad (11)$$

where the fluctuation in the total amount of surfactant S_f is defined as

$$S_f = [\Gamma_{12}g_1 + g_2 + \mathscr{Z}_2(H_{2,b} + m_{21}h_{12})]C_f + \mathscr{Z}_2C_b(H_{2,b}H_{2,f} + m_{21}h_{12}H_{1,f}). \quad (12)$$

The explicit expressions for the coefficients a_{ij} $(i,j = 1,2,3)$ are given in Appendix A [see eqs (A6)–(A14)]. Equations (9)–(11) form a system of three ordinary differential equations (ODE) governing the evolution of the perturbations in the film profile and in the surfactant concentration.

We chose the following initial conditions for the system of eqs (9)–(11):

(i) symmetric squeezing mode with amplitude ε compared to the initial hexane film thickness

$$H_{1,f}(0) = -\frac{\varepsilon}{2h_{12}}, \quad H_{2,f}(0) = \varepsilon \quad (13)$$

(ii) anti-symmetric bending mode with amplitude ε compared to the initial hexane film thickness

$$H_{1,f}(0) = \frac{\varepsilon}{h_{12}}, \quad H_{2,f}(0) = 0 \quad (14)$$

(iii) symmetric squeezing mode with amplitude ε compared to the initial water film thickness

$$H_{1,f}(0) = -\frac{\varepsilon}{2}, \quad H_{2,f}(0) = \varepsilon h_{12} \quad (15)$$

(iv) anti-symmetric bending mode with amplitude ε compared to the initial water film thickness

$$H_{1,f}(0) = \varepsilon. \quad H_{2,f}(0) = 0. \quad (16)$$

Here and hereafter we use $\varepsilon = 0.1$ in our numerical calculations.

The initial condition for the fluctuation in S_f is arbitrary from mathematical viewpoint. Physically, closer to the reality is the following assumption: the fluctuations in the total amount of species at the initial time are so fast, that the fluctuations in the bulk concentration at the initial moment is zero. Therefore, they are described by the fluctuations in the basic state for the adsorption and bulk concentration [see eq. (4)] and

$$S_f(0) = -\mathscr{Z}_2C_b(0)[H_{2,f}(0) + m_{21}h_{12}H_{1,f}(0)]. \quad (17)$$

The rupture time is defined as the time for which one of the films will rupture for a given wave number k. In all cases (i)–(iv) of initial conditions for interfacial shape and wave numbers k, we compute the rupture time t_r. The smallest value of t_r gives the life time of the system t_{cr}, the corresponding dimensionless critical film thickness $H_{2,cr}$ and the dimensionless critical wave number k_{cr}. In addition, we provide information which of the films has ruptured first.

4. NUMERICAL RESULTS FOR WATER–HEXANE FILM

We will consider here the particular system described in *Section 5* of Danov *et al.* (1997b), namely a two-layered water–hexane film sandwiched between a PVC substrate and hexane vapour. When the surfactant concentration is close or above CMC the surface elasticity and viscosity are high enough to prevent the tangential mobility of water–hexane interface and $U_{1,f} = 0$. This is the case that will be investigated in Section 4.1 below. For the liquid phases pure from surfactant, the interfacial velocities depend only on the pressure distribution (see Section 4.2). We will illustrate three different cases:

(A) dependence of the critical parameters on the initial hexane film thickness h_0 and on the temperature differences ΔT at given constant thickness h_w of the water film (see Figs 4 and 7);

(B) dependence of the critical parameters on the initial film thicknesses and ΔT for $h_0 = h_w$ (see Figs 5 and 8);

(C) dependence of the critical parameters on the initial hexane film thickness for very thin water layer $h_w = 5$ nm (see Figs 6 and 9).

The influence of surfactant at intermediate concentrations is illustrated in Section 4.3 below.

4.1. *Tangentially immobile water–hexane interface*

In the case, when the surfactant concentrations are above or close to CMC, $U_{1,f} = 0$. In this case, the hydrodynamic problem decouples from the surfactant

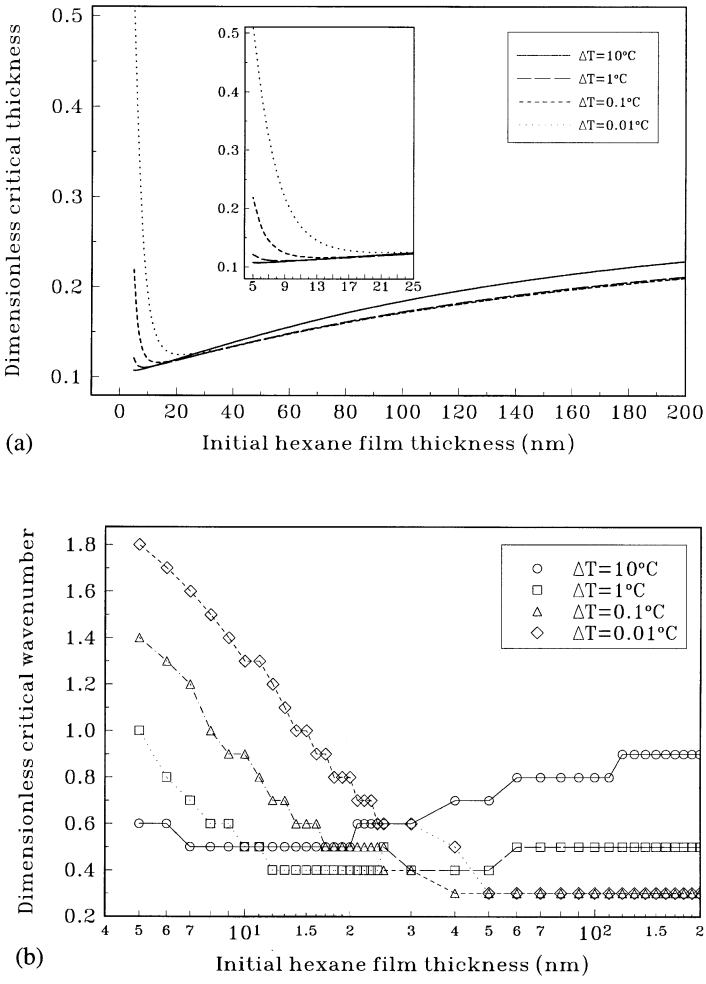

Fig. 4. Dependence of (a) the dimensionless critical hexane film thickness and (b) the dimensionless critical wave number for $h_w = 100$ nm on the initial hexane film thickness h_0. The temperature difference $\Delta T = 0.01$, 0.1, 1, and 10°C. The water–hexane interface is immobile.

mass balance (cf. Edwards *et al.*, 1991) and the linear system for the perturbations (9)–(11) reduces to a system of only two ODE for the amplitudes of the film shape fluctuations, as described in Appendix A [see eqs (A15)–(A17)]. For the numerical calculation of the corresponding initial-value problem we used the sixth-order Runge–Kutta numerical method with adaptive time step (IMSL, program DVERK) and numerical procedures for stiff systems of differential equations (cf. Press *et al.*, 1992). Unfortunately, these methods work with good precision only in the cases, when the coefficients are not much different in magnitude. For example, when the thicknesses are $h_0 = 5$ nm and $h_w = 20$ μm the coefficients are rather different, e.g. $a_{11} \propto 10^9$, $a_{12} \propto 10^6$, $a_{21} \propto 10^3$ and $a_{22} \propto 1$, and both numerical methods do not work at all. That is why we developed a new numerical procedure, which is described in the Appendix B.

In both cases (A) and (B) [see Figs 4(a) and 5(a)] when the initial thickness is greater than 20 nm, a greater initial thickness results in a greater dimensionless critical thickness. For temperature differences smaller than 1°C there is, in principle, no significant influence of ΔT on the critical thickness, but the film is more stable than the corresponding one at $\Delta T = 10$°C. For these thicknesses, the van der Waals effect is negligible. The temperature difference influences the critical wavelength for all investigated values [see Figs 4(b) and 5(b)]. The magnitude of the dimensionless critical wave number is in the order of unity and it can increase (for $\Delta T > 1$°C) or decrease (for $\Delta T < 1$°C) with increasing thickness. When the hexane film is thinner than 20 nm the influence of the molecular forces is significant for all temperature differences and it increases with decreasing of the temperature differences more than five times [see Figs 4(a) and 5(a)], i.e. with increasing of the disappearance time of the film. The van der Waals forces are stronger in this case, which leads to the decrease of the critical wavelength [see Figs 4(b) and 5(b)]. The higher temperature differences suppress the van der Waals forces. Finally, it is interesting to note that for all cases (A) and (B) the symmetric squeezing mode promotes the rupturing of the hexane film. It is not

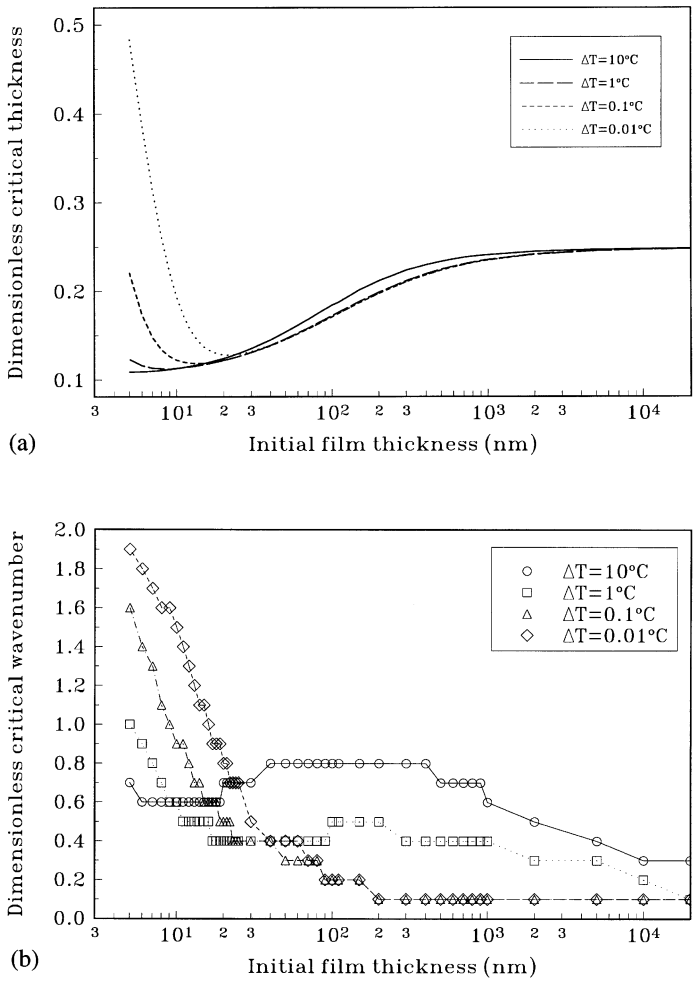

Fig. 5. Dependence of (a) the dimensionless critical hexane film thickness and (b) the dimensionless critical wave number on the initial film thickness. The initial film thicknesses of the water and hexane films are equal. The temperature difference ΔT is taken to be 0.01, 0.1, 1, and 10°C. The water–hexane interface is immobile.

a rule, because in the case (C) for very thin water layer, the antisymmetric bending mode is the time limiting factor.

When the water film is very thin (thinner than 20 nm) and the hexane film is thick enough (thicker than 7 μm) then the water film will rupture first due to the van der Waals attraction forces. In the case, when the water film will rupture, the dimensionless hexane film thickness increases from 0.3 to 0.95 with increase of the hexane film thickness to 20 μm (see Fig. 6). The critical wavelengths are much shorter compared with the other cases. The decreasing of the temperature difference makes the effect more pronounced.

4.2. *Pure water–hexane interface*

When the liquid phases are surfactant-free, the interfacial velocity depends only on the pressure distribution. The linear system for the perturbations (9)–(11) reduces again to a system of two ODE [see Appendix A for details, eqs (A18)–(A20)]. For numerical calculation, we use the corresponding initial conditions (13)–(16) and numerical method described in the Appendix B.

There are two factors acting in an opposite way compared to the case of tangentially immobile hexane–water interface: the higher surface tension stabilises the film; and due to the motion of the interface and the lateral temperature gradients the thermal Marangoni effect decreases the critical wave number, it increases the critical film thickness, and it acts destabilizing on the evaporating film.

In cases (A) and (B), the quantitative explanation of these effects is presented by Figs 7 and 8, where the critical thickness is illustrated as a function of the initial hexane film thickness for temperature differences $\Delta T = 0.01$, 0.1, 1, and 10°C. In contrast to the case of tangentially immobile hexane–water interface for large initial film thicknesses and sufficiently large temperature differences the thermal Marangoni effect produces additional destabilisation of the film, increasing the critical hexane film thickness. But due to the mobility of the hexane–vapour interface (the

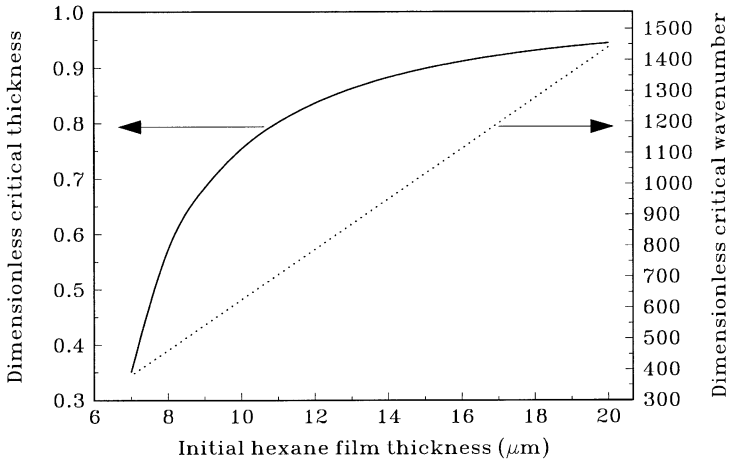

Fig. 6. Dependence of the dimensionless critical hexane film thickness and the critical wave number on the initial hexane film thickness h_0. The initial water film thickness is small, $h_w = 5$ nm. The temperature difference is $\Delta T = 10°C$. The interface water–hexane is immobile.

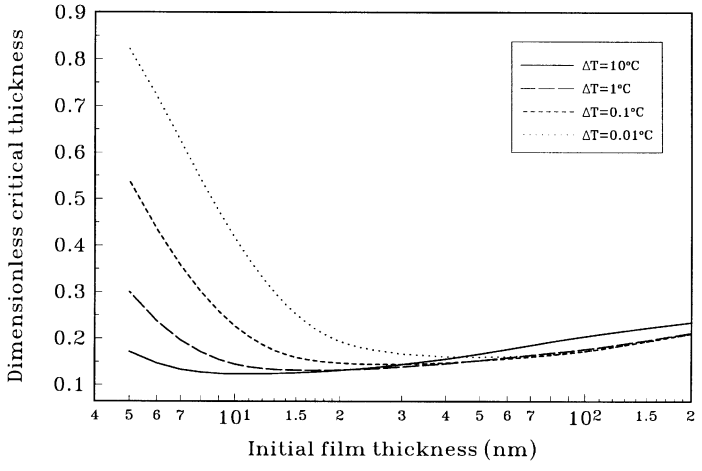

Fig. 7. Dependence of the dimensionless critical hexane film thickness on the initial film thickness h_0 for surfactant-free liquid layers. The initial water film thickness is $h_w = 100$ nm and the temperature difference ΔT is 0.01, 0.1, 1, and 10°C.

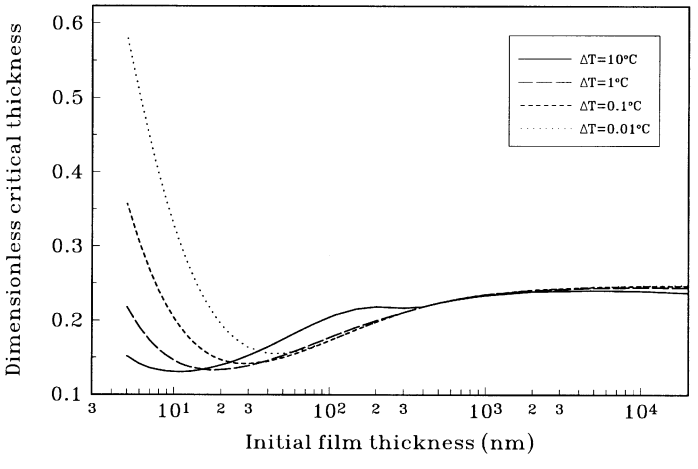

Fig. 8. Dependence of the dimensionless critical hexane film thickness on the initial film thickness for surfactant-free phases. The initial film thicknesses of the water and hexane phases are equal. The temperature difference ΔT is taken to be 0.01, 0.1, 1, and 10°C.

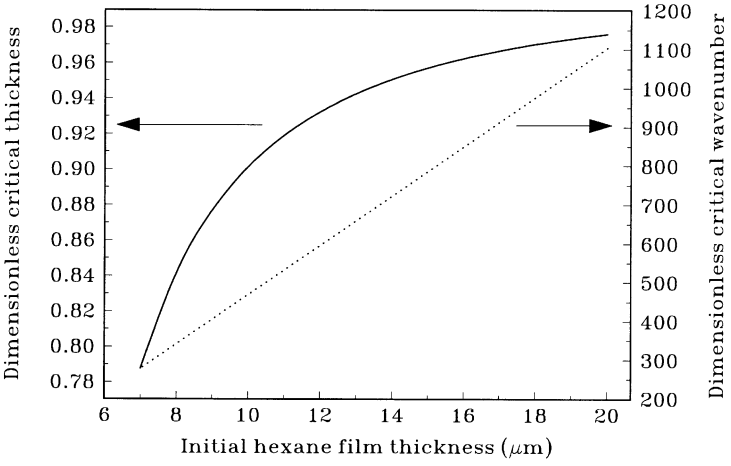

Fig. 9. Dependence of the dimensionless critical hexane film thickness and the critical wave number on the initial hexane film thickness h_0 for surfactant-free film phases. The initial water film thickness is small $h_w = 5$ nm and the temperature difference is $\Delta T = 10°C$.

surfactant cannot adsorb at this interface) this effect is not so significant as in the case of a single evaporating film (see Danov *et al.*, 1997a). For hexane film thickness smaller than 20 nm, where the van der Waals attraction plays an important role for the film stability, the interfacial mobility increases the critical thickness. The 2 times higher interfacial tension cannot prevent the evaporation, Marangoni and van der Waals instabilities, which leads to smaller film lifetime compared to the case of high surfactant concentration. The comparison between Figs 4(a) and 8 (case A) for $h_0 = 5$ nm and $\Delta T = 0.01°C$ shows an increase of the critical thickness from about 0.5 to 0.58. It is interesting to note that the comparison between Figs 5(a) and 8 (case B) does not lead to the same conclusion. In fact, the critical thicknesses for $h_0 = 5$ nm and $\Delta T = 0.01°C$ [Fig. 5(a)] and for $h_0 = h_w = 5$ nm and $\Delta T = 0.01°C$ (Fig. 8) are principally the same. This effect takes place because the thermal capacity of the 100 nm water layer is much higher than that of the 5 nm water film. Therefore, the evaporation intensity is lower and it cannot prevent the van der Waals instability. We observed that for large temperature difference at small thickness h_0 the longer waves destabilise the film contrary to the case of large thicknesses, where the critical wavelength is smaller [see Fig. 4(b)]. With decreasing temperature difference this affects directly opposite and the wave numbers decrease monotonically with increasing of the initial film thickness.

Our computations showed that for surfactant-free films in both cases (A) and (B), the symmetric squeezing mode promotes the rupturing of the hexane film.

In the case (C) when the water film is very thin (thinner than 20 nm) and the hexane film is thick enough (thicker than 7 μm) than the water film will also rupture first due to the van der Waals attraction forces as in Section 4.1. When the water film ruptures (Fig. 9), the dimensionless hexane film thickness is significantly higher than that in Fig. 6: it increases from 0.3 to 0.78 for $h_0 = 7$ μm and from 0.93 to 0.98 for the high initial hexane film thickness 20 μm. The critical waves are longer than in the case of high surfactant concentration. The decrease of the temperature difference makes the effect more pronounced. The anti-symmetric bending mode is again the time limiting factor.

4.3. *Influence of surfactant on the stability of P/W/H/V films*

In the case when the initial surfactant concentration is below critical micelles concentration, it is necessary to solve the full set of three equations (9)–(11) in order to calculate the film rupture time. For this purpose, we used the numerical method described in Appendix B. The initial conditions we use are given by eqs (13)–(14) and (17).

In order to illustrate the influence of surfactants on the stability of the evaporating hexane–water film we calculate the critical parameters in the case of a thin hexane film, $h_0 = 5$ nm, and the initial water layer thickness is 100 nm. The temperature differences were 0.01, 0.1, 1, and 10°C. We chose two different types of surfactant: low molecular weight surfactant [see Figs 10(a) and (b)] and high molecular weight surfactant [see Figs 10(c) and (d)]. It is shown that the increase of the temperature difference suppresses the influence of surfactant and there is no significant change of the film lifetime for all concentrations and types of surfactants. When the temperature difference is smaller than 1°C the transition from a fully mobile to an immobile hexane–water interface is well defined. In the transition zone, the critical thickness drops from values of surfactant-free layers to values of tangentially immobile interfaces. The solidification of the hexane–water interface for ionic surfactant is observed at an initial adsorption about 10^{-3}, since for high molecular weight surfactants it is found at an

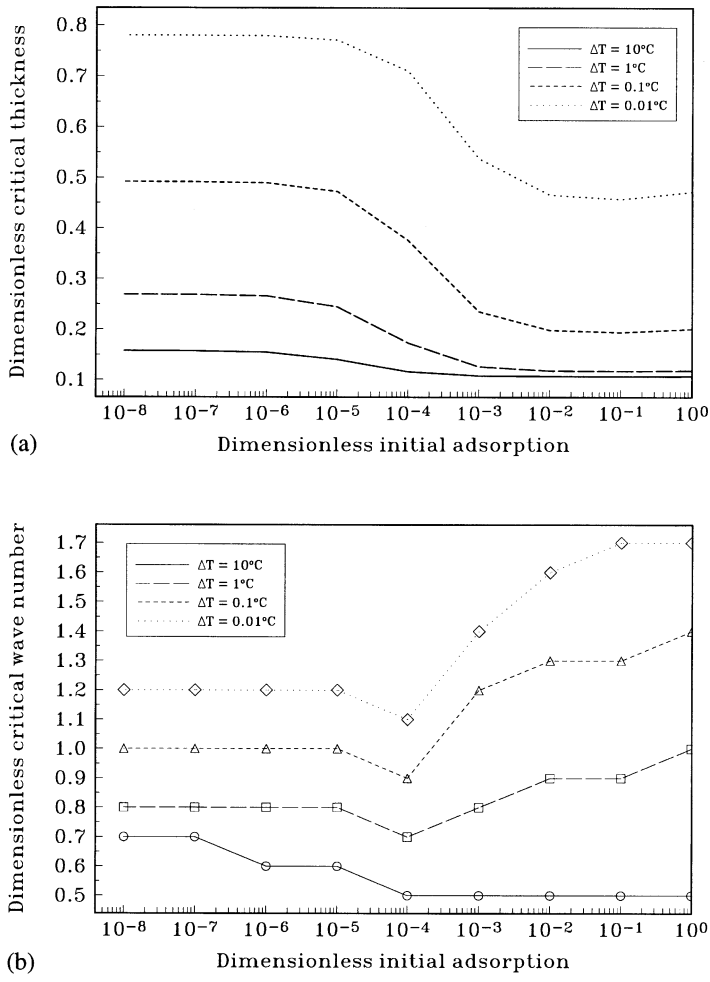

Fig. 10. Dependence of (a) the dimensionless critical hexane film thickness and (b) the dimensionless critical wave number on the initial adsorption of typical ionic surfactant. Dependence of (c) the dimensionless critical hexane film thickness and (d) the dimensionless critical wave number on the initial adsorption of typical high molecular weight surfactant. The initial film thicknesses are $h_0 = 5$ nm and $h_w = 100$ nm. The temperature difference ΔT is taken to be 0.01, 0.1, 1, and 10°C.

adsorption of about 10^{-6}, being three orders of magnitude lower [compare Figs 10(a) and (c)]. Therefore, the efficiency of high molecular weight surfactants is much higher than of the ionic one. Figures 10(b) and (d) show the decrease of the critical wavelength with increasing of the surfactant concentration for temperature differences lower than 1°C, where the surfactant affects the stability. The smaller the temperature difference is the higher the critical thickness is and therefore the van der Waals molecular forces are time limiting for the stability. For $\Delta T = 10$°C the evaporation and thermal Marangoni instabilities are the dominating factors.

When the initial film thicknesses are equal and not small, $h_0 = h_w = 100$ nm, the change of the critical film thickness is not so pronounced as in the previous case [compare Figs 10(a) and (c) and Figs 11(a) and (b)]. The solidification of the interface takes place at an adsorption one order of magnitude higher. It is a reasonable effect because the surfactants in our computations are chosen to be soluble in the water phase and their solubility in the hexane phase is 8 times lower. Therefore, the thicker hexane layer is a greater reservoir for the surfactant from the water phase and the solidification takes place at higher adsorption. The critical wavelengths have an opposite behaviour as in the previous case: the increase of the initial adsorption increases the critical wavelength. The critical thickness also changes in a different way: the increase of the temperature difference decreases slowly the relative stability of the films. Therefore, the evaporation and thermal Marangoni instabilities dominate the van der Waals destabilising effect.

Using this model and the numerical scheme, one can study many different cases. For example, when the water film is on the oil film and the surfactants are soluble in the different phases (see for details Paunov *et al.*, 1997). On the other hand, the van der Waals forces can be both positive or negative and can have stabilising or destabilising effects. Moreover, the

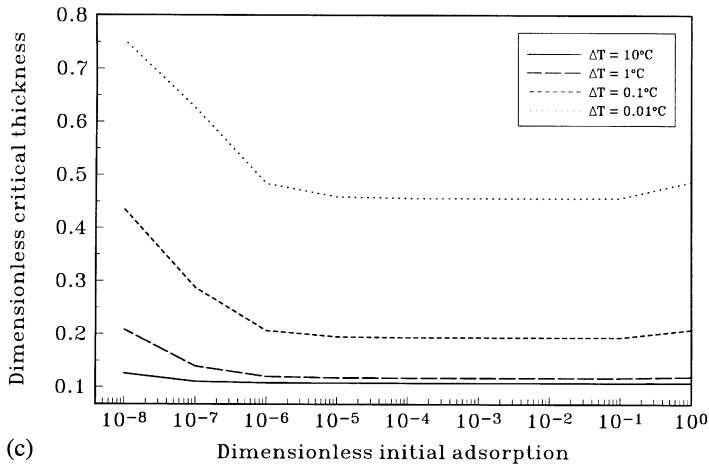

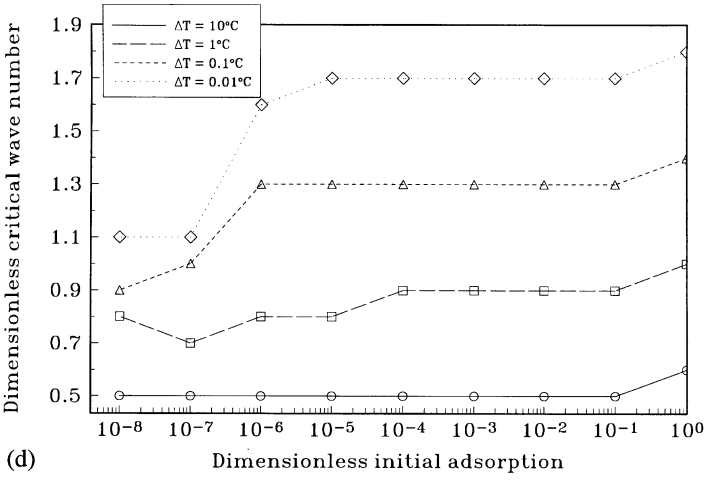

Fig. 10. (*Continued*).

influence of electrostatic, steric and other specific interaction is necessary to be taken into account for a given system. This makes the problem more complex and depending on the concrete physical system.

5. CONCLUSIONS

Linear stability analysis of evaporating two-layered liquid film on a heated solid substrate in the presence of surfactant is performed. The model is based on the general solution previously obtained by Danov *et al.* (1997b) using lubrication approximation. Both the instabilities due to thermal and surfactant Marangoni effects, coupled by the solvent mass loss are considered. The effect of the van der Waals surface force is also taken into account. The main results of this study are the following:

- Linear analysis of the stability of a particular system (water–hexane film upon a horizontal PVC substrate) against fluctuations has been performed. Three different cases are considered: the surfactant-free liquid layers, tangentially immobile water–hexane interface (a lot of surfactant), and the case of intermediate surfactant concentrations.
- We investigate the influence of different factors on the film stability: the tangential mobility of the film surfaces; the evaporation intensity; the initial thicknesses of the two layers, and the surfactant adsorption.
- The results from the linear analysis of the stability of water–hexane film show that in most cases the film shape fluctuations in *squeezing mode* give smaller rupture time than these in *bending mode*. Only for the case of ultra-thin water film (thinner than 20 nm) and thick hexane film (thicker than 7 μm), the bending mode leads to rupture of the water film.
- The presence of the second layer increase the film stability because of the increased thermal capacity of the whole film which decreases the relative evaporation intensity and suppresses instability due to the solvent mass loss.
- Two factors govern the film stability in the case of tangentially immobile interfaces: the higher surface tension stabilises the film, and due to the motion of interface and the lateral temperature gradients the

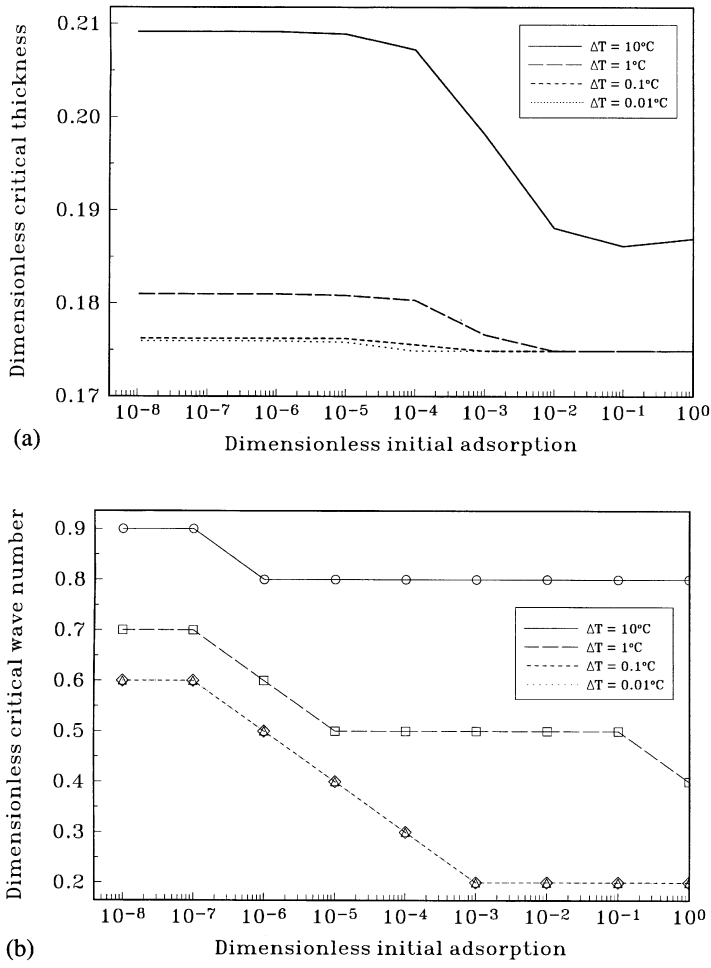

Fig. 11. Dependence of the dimensionless critical hexane film thickness on the initial adsorption of a typical (a) low molecular weight surfactant and (b) high molecular weight surfactant. The initial film thicknesses are equal and $h_w = h_0 = 100$ nm. The temperature difference ΔT is taken to be 0.01, 0.1, 1, and 10°C.

thermal Marangoni effect decreases the critical wave number, increases the critical film thickness, and it acts destabilising on the evaporating film.

- In the case of surfactant free film, for large initial film thicknesses and large temperature difference the thermal Marangoni effects produces additional destabilisation of the film, increasing the critical hexane film thickness. However, this effect is not as significant as in the case of single evaporating film [see Danov *et al.* 1997a)] due to the mobility of the hexane–vapour interface.
- For intensive evaporation the influence of surfactant is not so pronounced but when the temperature difference is smaller than 1°C the transition from a fully mobile to an immobile hexane–water interface is well established. The solidification of the hexane–water interface for high molecular weight surfactant is observed at three orders of magnitude lower adsorption than that of the ionic one.

We believe that this study can help for a better understanding of the physics of the stability of multi-layered films and can be useful for determining of the main factors that influence the film behaviour in particular systems.

Acknowledgements

This work was financially supported by the 'Volkswagen-Stiftung'. The authors gratefully acknowledge the support of their collaborative research.

REFERENCES

Danov, K. D., Alleborn, N., Raszillier, H. and Durst, F. (1998a) The stability of evaporating thin liquid films in the presence of surfactant: I. Lubrication approximation and linear analysis. *Phys. Fluids* **10** (1), 131–143.

Danov, K. D., Paunov, V. N., Alleborn, N., Raszillier, H. and Durst, F. (1997b) Stability of the evaporating two-layered liquid film in the presence of surfactant: I. The equations of lubrication approximation. *Chem. Engng Sci.* **53**, 2809–2822

Edwards, D. A., Brenner, H. and Wasan, D. T. (1991) *Interfacial Transport Processes and Rheology*. Butterworth-Heinemann, Boston, U.S.A.

IMSL - program library. Program DVERK.
Korn, G. A. and Korn, T. M. (1968). *Mathematical Handbook*. McGraw-Hill, New York, U.S.A.
Paunov, V. N., Danov, K. D., Alleborn, N., Raszillier, H. and Durst, F. (1997) Stability of the evaporating two-layered liquid film in the presence of surfactant: III. Non-linear stability analysis. *Chem. Engng Sci.* **53**, 2839–2857.
Press, W. H., Teukolsky, S. A., Vetterling, W. T. and Flannery, B. P. (1992) *Numerical Recipes in Fortran. The Art of Scientific Computing*. Cambridge University Press, Cambridge.

APPENDIX A. DERIVATION OF THE LINEAR PROBLEM EVOLUTION EQUATIONS

By substituting eq. (5) into the dimensionless form of the normal stress balance, [eqs (52) and (53) in Danov *et al.* (1997b)] and linearisation around the basic state (see Section 2) we obtain eq. (6) where the coefficients are as follows:

$$p_{h,21} = -\frac{\mathscr{E}\mathscr{K}^2 h_{12}\lambda_{21}}{2(\mathscr{K}+H_{2,b}+h_{12}\lambda_{21})^3} - \frac{\mathscr{W}_i h_{12}}{2(H_{2,b}+h_{12})^4} + \frac{k^2 h_{12}}{4}\left[1-\mathscr{S}_2\frac{\ln(1-\mathscr{G}_2 G_{2,b})}{\ln(1-\mathscr{G}_2)}\right] \tag{A1}$$

$$p_{h,22} = -\frac{\mathscr{E}\mathscr{K}^2 H_{2,b}}{2(\mathscr{K}+H_{2,b}+h_{12}\lambda_{21})^3} - \frac{\mathscr{W}_2}{2H_{2,b}^3} - \frac{\mathscr{W}_i H_{2,b}}{2(H_{2,b}+h_{12})^4} + \frac{k^2 H_{2,b}}{4}\left[1-\mathscr{S}_2\frac{\ln(1-\mathscr{G}_2 G_{2,b})}{\ln(1-\mathscr{G}_2)}\right] \tag{A2}$$

$$p_{h,11} = \frac{p_{h,21}}{\eta_{12}} - \frac{\mathscr{W}_1}{2\eta_{12}h_{12}^3} + \frac{k^2\sigma_{12}h_{12}}{4\eta_{12}}\left[1-\mathscr{S}_1\frac{\ln(1-\mathscr{G}_1 G_{1,b})}{\ln(1-\mathscr{G}_1)}\right] \tag{A3}$$

$$p_{h,12} = \frac{p_{h,22}}{\eta_{12}} + \frac{\mathscr{W}_2}{2\eta_{12}H_{2,b}^3}. \tag{A4}$$

Besides, we use eq. (5) to linearise the tangential stress balance [eqs (55) and (57) in Danov *et al.* (1997b)]. Thus, we obtain eq. (7), where the respective coefficients are

$$u_{h,11} = \frac{f_{v,2}v_{h,11}+v_{h,21}}{f_{v,1}f_{v,2}-1}, \quad u_{h,21} = \frac{f_{v,2}v_{h,12}+v_{h,22}}{f_{v,1}f_{v,2}-1},$$
$$u_{c,1} = \frac{f_{v,2}v_{c,1}+v_{c,2}}{f_{v,1}f_{v,2}-1}, \quad u_{h,21} = \frac{v_{h,11}+f_{v,1}v_{h,21}}{f_{v,1}f_{v,2}-1},$$
$$u_{h,22} = \frac{v_{h,12}+f_{v,1}v_{h,22}}{f_{v,1}f_{v,2}-1}, \quad u_{c,2} = \frac{v_{c,1}+f_{v,1}v_{c,2}}{f_{v,1}f_{v,2}-1}. \tag{A5}$$

Here, for the sake of brevity, we have introduced the notations:

$$f_{v,1} = 1+\frac{\eta_{12}}{h_{12}}H_{2,b}+k^2\mathscr{V}_1 H_{2,b}G_{1,b}, \quad f_{v,2} = 1+k^2\mathscr{V}_2 H_{2,b}G_{2,b}$$

$$v_{h,11} = 3k\eta_{12}h_{12}H_{2,b}p_{h,11} + 3kH_{2,b}^2 p_{h,21} - \frac{2k\mathscr{M}_1 h_{12}\lambda_{21}H_{2,b}(\mathscr{K}+H_{2,b})}{(\mathscr{K}+H_{2,b}+h_{12}\lambda_{21})^2}$$

$$v_{h,12} = 3k\eta_{12}h_{12}H_{2,b}p_{h,12} + 3kH_{2,b}^2 p_{h,22} + \frac{2k\mathscr{M}_1 h_{12}\lambda_{21}H_{2,b}^2}{(\mathscr{K}+H_{2,b}+h_{12}\lambda_{21})^2}$$

$$v_{c,1} = \frac{2k\mathscr{A}_1 g_1 H_{2,b}}{1-\mathscr{G}_1 G_{1,b}}, \quad v_{c,2} = \frac{2k\mathscr{A}_2 g_2 H_{2,b}}{1-\mathscr{G}_2 G_{2,b}}$$

$$v_{h,21} = 3kH_{2,b}^2 p_{h,21} - \frac{2k\mathscr{K}\mathscr{M}_2 h_{12}\lambda_{21}H_{2,b}}{(\mathscr{K}+H_{2,b}+h_{12}\lambda_{21})^2}$$

$$v_{h,22} = 3kH_{2,b}^2 p_{h,22} - \frac{2k\mathscr{K}\mathscr{M}_2 H_{2,b}^2}{(\mathscr{K}+H_{2,b}+h_{12}\lambda_{21})^2}.$$

By substituting of eqs (5)–(7) and (12) into the governing equations, [see eqs (44), (45) and (59) in Danov *et al.* (1997b)] and keeping only the leading terms we arrive at the system of ordinary differential equations (9)–(11), where the coefficients are defined as follows:

$$a_{11} = -k^2h_{12}^2 p_{h,11} - ku_{h,11} - a_{13}\mathscr{Z}_2 C_b m_{21}h_{12} \tag{A6}$$

$$a_{12} = -k^2h_{12}^2 p_{h,12} - ku_{h,12} - a_{13}\mathscr{Z}_2 C_b H_{2,b} \tag{A7}$$

$$a_{13} = -\frac{ku_{c,1}}{[\Gamma_{12}g_1+g_2+\mathscr{Z}_2(H_{2,b}+m_{21}h_{12})]} \tag{A8}$$

$$a_{21} = -k^2H_{2,b}^2 p_{h,21} - k(u_{h,11}+u_{h,21}) - a_{23}\mathscr{Z}_2 C_b m_{21}h_{12} + \frac{h_{12}\lambda_{21}}{2H_{2,b}}\cdot\frac{2\mathscr{K}+1+2h_{12}\lambda_{21}}{(\mathscr{K}+H_{2,b}+h_{12}\lambda_{21})^2} \tag{A9}$$

$$a_{22} = -k^2H_{2,b}^2 p_{h,22} - k(u_{h,12}+u_{h,22}) - a_{23}\mathscr{Z}_2 C_b H_{2,b} + \frac{\mathscr{K}+2H_{2,b}+h_{12}\lambda_{21}}{2H_{2,b}}\cdot\frac{2\mathscr{K}+1+2h_{12}\lambda_{21}}{(\mathscr{K}+H_{2,b}+h_{12}\lambda_{21})^2} \tag{A10}$$

$$a_{23} = -\frac{k(u_{c,1}+u_{c,2})}{[\Gamma_{12}g_1+g_2+\mathscr{Z}_2(H_{2,b}+m_{21}h_{12})]} \tag{A11}$$

$$a_{31} = -ku_{h,11}[2\Gamma_{12}G_{1,b}+\mathscr{Z}_2 C_b(H_{2,b}+m_{21}h_{12})] - a_{33}\mathscr{Z}_2 C_b m_{21}h_{12} - ku_{h,21}(2G_{2,b}+\mathscr{Z}_2 C_b H_{2,b}) - k^2\mathscr{Z}_2 C_b(m_{21}h_{12}^3 p_{h,11}+H_{2,b}^3 p_{h,21}) \tag{A12}$$

$$a_{32} = -ku_{h,12}[2\Gamma_{12}G_{1,b}+\mathscr{Z}_2 C_b(H_{2,b}+m_{21}h_{12})] - a_{33}\mathscr{Z}_2 C_b H_{2,b} - ku_{h,22}(2G_{2,b}+\mathscr{Z}_2 C_b H_{2,b}) - k^2\mathscr{Z}_2 C_b(m_{21}h_{12}^3 p_{h,12}+H_{2,b}^3 p_{h,22}) \tag{A13}$$

$$a_{33} = -\{k^2\mathscr{B}[\Gamma_{12}\mathscr{I}_1 g_1+\mathscr{I}_2 g_2+\mathscr{Z}_2(H_{2,b}+m_{21}h_{12}D_{12})] + ku_{c,1}[2\Gamma_{12}G_{1,b}+\mathscr{Z}_2 C_b(H_{2,b}+m_{21}h_{12})] + ku_{c,2}[2G_{2,b}+\mathscr{Z}_2 C_b H_{2,b})\}/[\Gamma_{12}g_1+g_2 + \mathscr{Z}_2(H_{2,b}+m_{21}h_{12})]. \tag{A14}$$

For the case of a tangentially immobile water–hexane interface and a fully mobile hexane–vapour surface the linear stability problem reduces to a system of two ordinary differential equations (9) and (10) where the corresponding expressions for the coefficients a_{ij} are

$$a_{11} = -k^2h_{12}^2 p_{h,11}, \quad a_{12} = -k^2h_{12}^2 p_{h,12}, \quad a_{13} = 0, \quad a_{23} = 0 \tag{A15}$$

$$a_{21} = -k^2H_{2,b}^2 p_{h,21} - kv_{h,21} + \frac{h_{12}\lambda_{21}}{2H_{2,b}} \times\frac{2\mathscr{K}+1+2h_{12}\lambda_{21}}{(\mathscr{K}+H_{2,b}+h_{12}\lambda_{21})^2} \tag{A16}$$

$$a_{22} = -k^2H_{2,b}^2 p_{h,22} - kv_{h,22} + \frac{\mathscr{K}+2H_{2,b}+h_{12}\lambda_{21}}{2H_{2,b}} \times\frac{2\mathscr{K}+1+2h_{12}\lambda_{21}}{(\mathscr{K}+H_{2,b}+h_{12}\lambda_{21})^2}. \tag{A17}$$

The definitions of all others coefficients are the same as in the general case, eqs (A1)–(A5), with the setting of $G_{1,b} = 1$ and $G_{2,b} = 0$.

In the case of surfactant-free liquid phases, the linear stability problem reduces again to a system of two ODE (9) and (10) where the coefficients a_{ij} have the following form:

$$a_{11} = -k^2 h_{12}^2 p_{h,11} - k u_{h,11}, \quad a_{12} = -k^2 h_{12}^2 p_{h,12} - k u_{h,12},$$
$$a_{13} = 0, \quad a_{23} = 0 \tag{A18}$$

$$a_{21} = -k^2 H_{2,b}^2 p_{h,21} - k(u_{h,11} + u_{h,21}) + \frac{h_{12}\lambda_{21}}{2H_{2,b}} \times \frac{2\mathscr{K} + 1 + 2h_{12}\lambda_{21}}{(\mathscr{K} + H_{2,b} + h_{12}\lambda_{21})^2} \tag{A19}$$

$$a_{22} = -k^2 H_{2,b}^2 p_{h,22} - k(u_{h,12} + u_{h,22}) + \frac{\mathscr{K} + 2H_{2,b} + h_{12}\lambda_{21}}{2H_{2,b}} \cdot \frac{2\mathscr{K} + 1 + 2h_{12}\lambda_{21}}{(\mathscr{K} + H_{2,b} + h_{12}\lambda_{21})^2}. \tag{A20}$$

The definitions of all coefficients in eqs (A1)–(A5) are the same as in the general case with the concentration of surfactant and adsorption taken to be zero.

APPENDIX B. NUMERICAL METHOD FOR THE INITIAL -VALUE PROBLEM

We consider a linear system of n differential equations

$$\frac{\mathrm{d}f_i}{\mathrm{d}t} = \sum_{k=1}^{n} a_{ik}(t) f_k \quad (k = 1, 2, \ldots, n) \tag{B1}$$

in a small time interval $(t_0, t_0 + \Delta t)$ with initial conditions

$$f_k(t_0) = f_{k,0} \quad (k = 1, 2, \ldots, n). \tag{B2}$$

The exact solution of the problem (B1)–(B2) can be written in the matrix-exponential form

$$\mathbf{f}(t) = \exp\left[\int_{t_0}^{t} \mathbf{A}(\tau)\,\mathrm{d}\tau\right] \cdot \mathbf{f}(t_0) \tag{B3}$$

where the vector of solution is **f** and the matrix of coefficients is **A**. The integral appearing in eq. (B3) can be replaced by the trapezoidal rule

$$\mathbf{f}(t_0 + \Delta t) \propto \exp\left[\mathbf{A}\left(t_0 + \frac{\Delta t}{2}\right)\Delta t\right] \cdot \mathbf{f}(t_0) \tag{B4}$$

with precision Δt^3. The approximate solution (B4) is the solution of the corresponding system of differential equations with constant coefficients a_{ik}^0 at time $t_0 + \Delta t/2$, $a_{ik}^0 = a_{ik}(t_0 + \Delta t/2)$.

In the case of a system of two differential equations the characteristic values of the matrix ω_1 and ω_2 can be calculated from the expression

$$\omega_{1,2} = \tfrac{1}{2}[a_{11}^0 + a_{22}^0 \pm \sqrt{(a_{11}^0 - a_{22}^0)^2 + 4a_{12}^0 a_{21}^0}]. \tag{B5}$$

In our computation the characteristic values are real and different. Therefore, the approximate solution at $t_0 + \Delta t$ is

$$f_1(t_0 + \Delta t) = \left(\frac{\omega_2 - a_{11}^0}{\omega_2 - \omega_1} f_{1,0} - \frac{a_{12}^0}{\omega_2 - \omega_1} f_{2,0}\right)\exp(\omega_1 \Delta t) + \left(\frac{a_{11}^0 - \omega_1}{\omega_2 - \omega_1} f_{1,0} + \frac{a_{12}^0}{\omega_2 - \omega_1} f_{2,0}\right)\exp(\omega_2 \Delta t)$$

$$f_2(t_0 + \Delta t) = \left(-\frac{a_{21}^0}{\omega_2 - \omega_1} f_{1,0} - \frac{\omega_1 - a_{11}^0}{\omega_2 - \omega_1} f_{2,0}\right)\exp(\omega_1 \Delta t) + \left(\frac{a_{21}^0}{\omega_2 - \omega_1} f_{1,0} + \frac{\omega_2 - a_{11}^0}{\omega_2 - \omega_1} f_{2,0}\right)\exp(\omega_2 \Delta t). \tag{B6}$$

In the case of a system of three differential equations the characteristic values are calculated as a solution of the equation

$$\omega^3 + a\omega^2 + b\omega + c = 0 \tag{B7}$$

where the coefficients a, b, and c are defined by the following expressions:

$$a = -(a_{11}^0 + a_{22}^0 + a_{33}^0)$$
$$b = a_{11}^0 a_{22}^0 - a_{12}^0 a_{21}^0 + a_{11}^0 a_{33}^0 - a_{13}^0 a_{31}^0 + a_{22}^0 a_{33}^0 - a_{23}^0 a_{32}^0 \tag{B8}$$
$$c = -\det(a_{ik}^0).$$

The solution of (B7) we can represent using the Cardano formulas (cf. Korn and Korn, 1968)

$$p = b - \frac{a^2}{3}, \quad q = 2\left(\frac{a}{3}\right)^3 - \frac{ab}{3} + c, \quad r = \left(\frac{p}{3}\right)^3 + \left(\frac{q}{2}\right)^2$$
$$\alpha = \sqrt[3]{-\frac{q}{2} + \sqrt{r}}, \quad \beta = -\frac{p}{3\alpha}$$
$$\omega_1 = -\frac{a}{3} + \alpha + \beta, \quad \omega_{2,3} = -\frac{a}{3} - \frac{\alpha + \beta}{2} \pm i(\alpha - \beta)\frac{\sqrt{3}}{2}. \tag{B9}$$

In our case the characteristic values are real and the approximate solution (B4) can be written as follows: (i) for different characteristic values

$$f_k(t_0 + \Delta t) = C_{1k}\exp(\omega_1 \Delta t) + C_{2k}\exp(\omega_2 \Delta t) + C_{3k}\exp(\omega_3 \Delta t) \tag{B10a}$$

(ii) for two equal characteristic values $\omega_1 \neq \omega_2 = \omega_3$

$$f_k(t_0 + \Delta t) = C_{1k}\exp(\omega_1 \Delta t) + (C_{2k} + C_{3k}\Delta t)\exp(\omega_2 \Delta t) \tag{B10b}$$

and (iii) if all characteristic values are equal to ω_1 then

$$f_k(t_0 + \Delta t) = (C_{1k} + C_{2k}\Delta t + C_{3k}\Delta t^2)\exp(\omega_1 \Delta t) \tag{B10c}$$

where $(k = 1, 2, 3)$. The constants, appearing in formulas (B10) are the solution of the linear systems of initial conditions

$$\sum_{j=1}^{3} B_{ij} C_{jk} = F_{ik} \quad (i, k = 1, 2, 3). \tag{B11}$$

The right-hand side of eq. (B11) depends on the corresponding initial value of the problem and

$$F_{1k} = f_{k,0}, \quad F_{2k} = a_{k1}^0 f_{1,0} + a_{k2}^0 f_{2,0} + a_{k3}^0 f_{3,0}$$
$$F_{3k} = \sum_{i=1}^{3}\sum_{j=1}^{3} a_{ki}^0 a_{ij}^0 f_{j,0} \quad (k = 1, 2, 3). \tag{B12}$$

The matrix **B** of the system (B11) is defined, depending on the type of characteristic values:

(i) for different characteristic values

$$\mathbf{B} = \begin{Vmatrix} 1 & 1 & 1 \\ \omega_1 & \omega_2 & \omega_3 \\ \omega_1^2 & \omega_2^2 & \omega_3^2 \end{Vmatrix} \tag{B13a}$$

(ii) for two equal characteristic values $\omega_1 \neq \omega_2 = \omega_3$

$$\mathbf{B} = \begin{Vmatrix} 1 & 1 & 0 \\ \omega_1 & \omega_2 & 1 \\ \omega_1^2 & \omega_2^2 & 2\omega_2 \end{Vmatrix} \tag{B13b}$$

(iii) if all characteristic values are equal to ω_1 then

$$\mathbf{B} = \begin{Vmatrix} 1 & 0 & 0 \\ \omega_1 & 1 & 0 \\ \omega_1^2 & 2\omega_1 & 2 \end{Vmatrix}. \tag{B13c}$$

In principle, this algorithm can be used for systems with n differential equations, but the difficulties lie in the computation of the exact solution.